J|A|C|S COMMUNICATIONS

Published on Web 03/19/2010

Comparison of Solid-State Dipolar Couplings and Solution Relaxation Data Provides Insight into Protein Backbone Dynamics

Veniamin Chevelkov,[†,‡] Yi Xue,[‡] Rasmus Linser,[†] Nikolai R. Skrynnikov,[*,‡] and Bernd Reif[*,†]

Forschunginstitut für Molekulare Pharmakologie (FMP), Robert-Rössle-Strasse 10, 13125 Berlin, Germany, and Department of Chemistry, Purdue University, 560 Oval Drive, West Lafayette, Indiana 47907-2084

Received November 19, 2009; Revised Manuscript Received January 24, 2010; E-mail: nikolai@purdue.edu; reif@fmp-berlin.de

Internal motions on the scale of 10 ns−10 μs fall in a "blind spot" of solution NMR experiments traditionally used for studies of protein dynamics.[1] Recently, a new experimental strategy has emerged to probe these motions. In this new approach, the generalized order parameters derived from conventional ^{15}N relaxation data are compared with their counterparts extracted from $^{1}H^{N}-^{15}N$ residual dipolar couplings.[2,3] This method, however, is rather demanding in the part involving residual dipolar couplings (rDCs). The complete analysis of rDC requires a separation of structural and dynamic variables, as well as the variables pertaining to protein alignment in the orienting media. The success is dependent on the availability of accurate data from multiple aligned samples which need to be significantly different (orthogonal). Furthermore, the degree of alignment A_a proves to be "entangled" with the amplitude of the (axially symmetric) internal motion, which makes it difficult to separate the two quantities. To address this situation, rDC-based order parameters have been scaled in relation to the relaxation-based order parameters.[4] Recently, backbone rDCs such as $^{13}C'-^{13}C^{\alpha}$ have been used to establish the scaling factor (corresponding dipolar vectors can be considered rigid or near-rigid for secondary-structure residues in small globular proteins).[5,6]

In this communication we propose an alternative approach where the solution-state rDC data are replaced with the solid-state DC data. Similar to rDC-based order parameters, DC-based order parameters absorb motions on a sub-μs time scale. At the same time, the DC data have two critical advantages: (*i*) for protein molecules immobilized in the crystalline lattice the alignment tensor is known *a priori*[7] and (*ii*) in a polycrystalline sample all vectors are rendered spatially equivalent as a consequence of powder averaging. Thus, the alignment variables and structural variables, which cause so much trouble in the analyses of dynamics using rDCs, do not enter into consideration in the case of the DC-based analyses.

The idea of comparing the DC-based order parameters, S^2_{DC}, with the solution relaxation-based order parameters, S^2_{rel}, has been explored before.[8] In this work, however, we benefit from the improved accuracy of the DC measurements.[9] The advantage stems from the use of a perdeuterated protein sample with only 10% of protons back-substituted into exchangeable sites. For a small, well-behaved protein such as α-spectrin SH3 domain,[10] this labeling scheme leads to high-quality spectra[11] which, in turn, translate into more accurate DC data. It also helps that in the heavily deuterated sample one does not need to be concerned about proton−proton couplings.[12] The CPPI recoupling sequence[13] employed in our experiment is remarkably stable with respect to rf field mismatch and inhomogeneity, which further contributes to the accuracy of the measurements. Finally, certain progress has been made on the interpretation side; e.g., the proton isotropic chemical shift has been explicitly included in the simulations.[9] As a result of all these improvements, the estimated average error in the DCs has been cut to the level of ca. 3%.[14] This compares favorably with the previous body of work where the errors were in excess of 5% and usually close to 10%. This kind of improvement is critical for the analysis of the DC-derived order parameters, which are normally confined to a relatively narrow range.

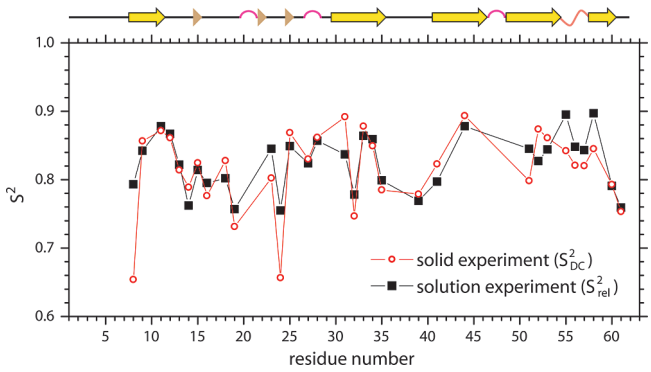

Figure 1. Experimentally determined order parameters in α-spectrin SH3. The solid- and solution-state data sets have been analyzed independently using the standard values for the NH bond length, r_{NH} = 1.02 Å, and the ^{15}N CSA anisotropy, −172 ppm. Using the more accurate estimate for the effective bond length, 1.015 Å,[5] leads to a trivial downward shift in the S^2_{DC} and S^2_{rel} profiles (1.5% and ∼2.3%, respectively). Only those residues for which both solid and solution data are available are shown in the plot (see Table S1 for complete list of data).

The solid-state DC data described above were converted into order parameters, S^2_{DC}, using the simple relationship $D_i = S_{DC}D_{max}$, where $D_{max} = -(1/2\pi)(\mu_0/4\pi)\gamma_H\gamma_N\hbar/r^3_{NH}$. Note that this approach ignores the anisotropy of local motion, which does not manifest itself in our experimental data[9] (see Supporting Information for detailed discussion). Separately and independently, ^{15}N relaxation data from our previous solution-state study (R_1, R_2, NOE measured at 500 and 600 MHz field strengths)[15] were analyzed by means of the standard two-parameter Lipari−Szabo model.[16] The resulting fast-motion parameters are typical of a small globular protein such as α-spectrin SH3 (mean S^2_{rel} = 0.83, τ_e = 27 ps).

Figure 1 illustrates the comparison between the solid-state S^2_{DC} and solution S^2_{rel}. The agreement between the two independently obtained series of order parameters is remarkable. Aside from the two residues, Leu-8 and Thr-24, S^2_{DC} and S^2_{rel} values are nearly identical, strongly suggesting that most amide sites do not experience any significant motions on the ns−μs time scale.[17]

This picture is consistent with the consensus that has recently emerged in the field. Specifically, the rDC data from select globular proteins (ubiquitin and GB3) suggest that there is very little or no ns−μs motions in the protein backbone−aside from termini and a

[†] Forschunginstitut für Molekulare Pharmakologie.
[‡] Purdue University.

handful of mobile loops.[3,6] This notion is also in agreement with early relaxation studies that focused on ns dynamics.[18]

Of special interest for us is comparing the results in Figure 1 with our previous findings based on the combination of solution- and solid-state relaxation data. In particular, we recently analyzed a large set of ^{15}N data from the α-spectrin SH3 domain, which included the solid-state R_1 rates measured at 600 and 900 MHz.[15] The analysis, using a variant of the extended Lipari−Szabo model, allowed us to probe the motions on the time scale ∼1−100 ns. As it turned out, for 19 out of 34 characterized residues the slow-motion order parameter $S^2_{rel,s}$ is greater than 0.97. Furthermore, for all but two residues $S^2_{rel,s}$ is greater than 0.92.[19] This result points toward the small amplitudes of ns motions, in agreement with the data shown in Figure 1. Considering residues Leu-8 and Thr-24 which show a significant difference between DC- and relaxation-based order parameters, Figure 1, both of them produced evidence of ns motion in our previous study ($S^2_{rel,s}$ equal to 0.92 and 0.93, respectively).[15] Similar observations can be made by analyzing the extended set of the solid-state data.[20]

In the absence of the overall tumbling, ns−μs local dynamics in solids can be highly efficient in causing spin relaxation, which in turn leads to line broadening and the ultimate disappearance of spectral peaks. In α-spectrin SH3, this happens to residues 1−7 from the disordered N-terminus, residues 36−38 from the so-called n-Src loop, and residues 47−48 from the distal loop. The corresponding spectral peaks are weak or missing in the current DC experiment which employs cross-polarization transfer (although some of them show up in the INEPT-based experiment; see Figure S1). Due to dynamic disorder, the N-terminal residues and several atoms in Asp-48 also cannot be resolved by X-ray crystallography.[21] Note that these observations fit the general pattern whereby ns−μs dynamics is concentrated in the loop regions and termini.

Dipolar relaxation effectively restricts the range of dynamics that can be probed through solid-state DCs (upper limit of several microseconds, Figure S2). In contrast, rDCs in solution impose no such restriction because they are typically 1000-fold smaller than DCs. In practice, rDCs can be used to study motions on the time scale extending to several milliseconds. There is, therefore, a potentially useful complementarity between the two types of data, with DCs being more selective of the two.

A meaningful comparison between S^2_{rel} and S^2_{DC} is predicated on the assumption that backbone dynamics does not change significantly upon protein crystallization.[15] To further explore this aspect, we undertook a series of MD simulations. Briefly, the crystallographic unit cell containing four protein molecules has been constructed (protein coordinates are from high-resolution structure 1U06; the dimensions of the orthorhombic unit cell are from room-temperature structure 2NUZ).[21] The cell was then hydrated and used as the initial structural model to record a 50-ns MD trajectory (CHARMM 32b2).[22] The simulation protocol was the same as previously described for the trajectory of α-spectrin SH3 in solution.[15,23] The only difference arises from the definition of the water box and the associated periodic boundary conditions: in one case the model recreates the crystal lattice environment, including multiple crystal contacts, while in the other case the protein is completely immersed in water.

The solid-state order parameters have been extracted from the MD trajectory as[24]

$$S^2 = (4\pi/5) \sum_{m=-2}^{2} \langle Y^*_{2m}(\Omega)\rangle\langle Y_{2m}(\Omega)\rangle \qquad (1)$$

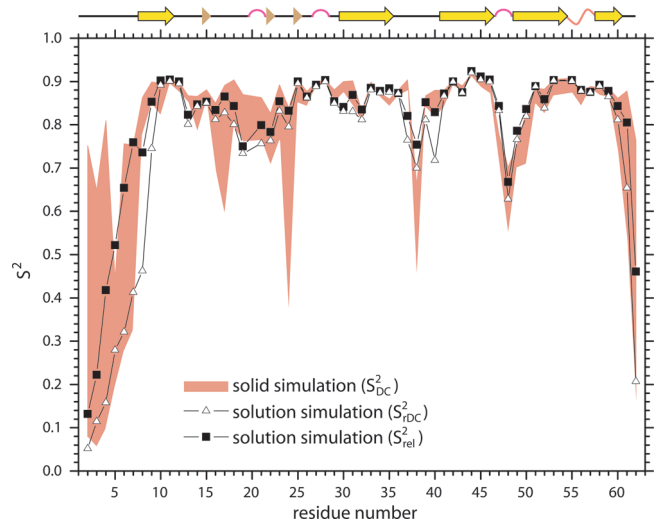

Figure 2. Simulated order parameters in α-spectrin SH3. Of note, the correlation coefficient between the simulated and experimental S^2_{DC} values turns out to be $r = 0.94$ (calculated for 44 residues for which the experimental solid-state data are available; simulated S^2_{DC} values have been averaged over four protein molecules in the unit cell).

where Ω describes the direction of the NH vector in the fixed crystal frame. So-defined order parameters absorb both ps and ns dynamics and therefore can be thought of as the analogue of S^2_{DC}. The range of the simulated S^2_{DC} values from the four protein molecules in the unit cell is represented with a pink shaded area in Figure 2. Equation 1 has also been applied to the solution MD data, post-processed to remove the effect of the protein's overall tumbling (simulated order parameters S^2_{rDC}; open triangles in Figure 2). Alternatively, the solution trajectory can be used to simulate the set of ^{15}N relaxation rates (comprised of the same data as the experimental data set), that are subsequently fitted with the Lipari−Szabo model. The resulting order parameters are equivalent to S^2_{rel} (black squares in Figure 2).

Even though the current MD trajectories are relatively short, they offer a number of interesting insights. Through most of the sequence the solution data show little or no ns dynamics (triangles vs squares), with the pattern of the order parameters similar to that observed in the hydrated crystal (shaded area). In addition, a number of observations pertaining to the specific sites can be made.

(*i*) In solution, the disordered N-terminus (residues 1−7) engages in large-amplitude motions on the ns time scale. In solids, these motions are hindered/slowed down by extensive crystal contacts. Consequently, large-scale transitions have been observed for some, but not all, of the four protein molecules comprising the crystallographic unit cell (resulting in a wide spread of S^2_{DC} values, Figure 2).

(*ii*) Residue Leu-8, which caps the β-sheet, is also affected. The solution trajectory shows that occasionally the hydrogen bond at this site becomes broken and Leu-8 starts behaving as a part of the disordered N-terminus. This explains the presence of ns−μs dynamics in this residue (Figure 1). In the crystalline environment, however, large fluctuations involving Leu-8 apparently become too infrequent and therefore do not register in the relatively short solid-state trajectory. In the case of the other dynamic residue, Thr-24, both solution and solid-state simulations reproduce the respective experimental parameters, S^2_{rel} and S^2_{DC}, reasonably well.

(*iii*) Curiously, the mobility of residue Asn-38 increases upon crystallization. As it turns out, the corresponding peptide plane jumps between two disparate orientations. One of the two conformations is somewhat strained ($\psi \approx 20°$ in Thr-37) and is not

favored in solution. In the crystal, however, this conformation is stabilized by the intermolecular hydrogen bonds formed by the side chain of Asn-38. This is an interesting example of how crystal contacts can lead to a local destabilization in the protein structure. Recall that residue 38 is unobservable in the solid-state DC experiment.

(*iv*) The presence of significant dynamics in the distal loop around Asp-48 is confirmed by the increased crystallographic B-factors. Residue Asn-47 assumes an unusual conformation ($\phi \approx 50°$, $\psi \approx -110°$)[25] which has a destabilizing effect on the structure.[26] Asp-48 is also the only residue featuring exchange broadening in solution ($R_{ex} = 28\ s^{-1}$ at 600 MHz).

It can be safely assumed that ns$-\mu$s dynamics in a protein backbone involves crossing energy barrier(s). For example, conformational rearrangements in short peptides involving transitions over multiple barriers in (ϕ, ψ)-space occur on this time scale.[27] In this sense ns$-\mu$s dynamics is similar to the extensively studied μs$-$ms dynamics. As it happens, μs$-$ms motions are rare in well-structured globular proteins. When such motions occur, they mostly involve loops,[28] as well as special situations like local unfolding,[29] disulfide or proline isomerization,[30] etc. We suggest that the same is true for ns$-\mu$s backbone motions$-$they are mostly confined to the loop regions and are unlikely to occur in the structured portion of a protein, e.g. in a β-pleated sheet.

Indeed, it is difficult to expect that a globular protein would alternate between two similar but distinct conformational states with appreciably different β-sheet geometries (i.e., significantly different orientations of peptide planes within the β-sheet). Such a scenario would be inconsistent with Anfinsen's dogma which suggests that the protein fold is unique.[31] While it is known that side chains are frequently engaged in rotameric jumps on the time scale >1 ns, recent studies show that these motions do not affect the structured portion of the backbone which "nearly always...stays within a single local energy well".[32]

In conclusion, our results suggest that comparative analysis of solution relaxation data and solid-state DCs can provide a surprisingly accurate picture of backbone dynamics. In particular, this approach can be used to access much-discussed ns$-\mu$s backbone motions. In this respect, solid-state DCs offer a new route compared to solution rDCs. Our data support the emerging point of view that ns$-\mu$s motions occur in mobile loops, termini, and side chains, but generally not in the structured portion of the backbone. Scaffolds such as the β-sandwich are apparently too stiff, exhibiting fast (ps) motions, but not conducive to slower dynamics. It is clear, however, that more proteins with different architectures need to be studied before any broad conclusions can be drawn.

Acknowledgment. This work was supported by the DFG grant Re1435 to B.R. and the NSF grant CHE-0723718 to N.R.S. We are grateful to Nathan Benjamin for his help with MD simulations.

Supporting Information Available: Solid-state spectra of α-spectrin SH3 domain; plot illustrating the range of $\{S^2,\tau\}$amenable to DC-based studies; equivalent of Figure 1 with indicated experimental uncertainties; complete table of S^2_{DC} and S^2_{rel} data; analysis of the effect of motional anisotropy on S^2_{DC}; description of the MD simulation protocol. This material is available free of charge via the Internet at http://pubs.acs.org.

References

(1) Palmer, A. G. *Chem. Rev.* **2004**, *104*, 3623.
(2) Tolman, J. R.; Al-Hashimi, H. M.; Kay, L. E.; Prestegard, J. H. *J. Am. Chem. Soc.* **2001**, *123*, 1416. Meiler, J.; Prompers, J. J.; Peti, W.; Griesinger, C.; Brüschweiler, R. *J. Am. Chem. Soc.* **2001**, *123*, 6098. Clore, G. M.; Schwieters, C. D. *Biochemistry* **2004**, *43*, 10678.
(3) Yao, L.; Vögeli, B.; Torchia, D. A.; Bax, A. *J. Phys. Chem. B* **2008**, *112*, 6045. Lange, O. F.; Lakomek, N. A.; Farès, C.; Schröder, G. F.; Walter, K. F. A.; Becker, S.; Meiler, J.; Grubmüller, H.; Griesinger, C.; de Groot, B. L. *Science* **2008**, *320*, 1471.
(4) Tolman, J. R. *J. Am. Chem. Soc.* **2002**, *124*, 12020. Lakomek, N. A.; Walter, K. F. A.; Farès, C.; Lange, O. F.; de Groot, B. L.; Grubmüller, H.; Brüschweiler, R.; Munk, A.; Becker, S.; Meiler, J.; Griesinger, C. *J. Biomol. NMR* **2008**, *41*, 139.
(5) Yao, L. S.; Vögeli, B.; Ying, J. F.; Bax, A. *J. Am. Chem. Soc.* **2008**, *130*, 16518.
(6) Salmon, L.; Bouvignies, G.; Markwick, P.; Lakomek, N.; Showalter, S.; Li, D. W.; Walter, K.; Griesinger, C.; Bruschweiler, R.; Blackledge, M. *Angew. Chem., Int. Ed.* **2009**, *48*, 4154.
(7) In principle, one should take into consideration a possibility of "rocking" motion of the protein in the crystal cell. There is, however, evidence that the amplitude of this motion is very small, on the order of 1° (Meinhold, L.; Smith, J. C. *Biophys. J.* **2005**, *88*, 2554). At this point we choose to disregard this motion.
(8) Cole, H. B. R.; Torchia, D. A. *Chem. Phys.* **1991**, *158*, 271. Lorieau, J. L.; McDermott, A. E. *J. Am. Chem. Soc.* **2006**, *128*, 11505. Yang, J.; Tasayco, M. L.; Polenova, T. *J. Am. Chem. Soc.* **2009**, *131*, 13690.
(9) Chevelkov, V.; Fink, U.; Reif, B. *J. Am. Chem. Soc.* **2009**, *131*, 14018.
(10) Castellani, F.; van Rossum, B.; Diehl, A.; Schubert, M.; Rehbein, K.; Oschkinat, H. *Nature* **2002**, *420*, 98.
(11) Chevelkov, V.; Rehbein, K.; Diehl, A.; Reif, B. *Angew. Chem., Int. Ed.* **2006**, *45*, 3878.
(12) Munowitz, M.; Aue, W. P.; Griffin, R. G. *J. Chem. Phys.* **1982**, *77*, 1686.
(13) Dvinskikh, S. V.; Zimmermann, H.; Maliniak, A.; Sandstrom, D. *J. Magn. Reson.* **2003**, *164*, 165. Dvinskikh, S. V.; Zimmermann, H.; Maliniak, A.; Sandstrom, D. *J. Chem. Phys.* **2005**, *122*, 044512.
(14) Includes random noise-type error (see Figure S1), as well as ca. 1% systematic error which originates mainly from site-to-site variations in the ^{15}N CSA anisotropy.[9]
(15) Chevelkov, V.; Zhuravleva, A. V.; Xue, Y.; Reif, B.; Skrynnikov, N. R. *J. Am. Chem. Soc.* **2007**, *129*, 12594.
(16) Lipari, G.; Szabo, A. *J. Am. Chem. Soc.* **1982**, *104*, 4546.
(17) It is assumed that internal protein dynamics in a well-hydrated protein crystal is quantitatively similar to dynamics in solution, notwithstanding the effect of crystal contacts (Agarwal, V.; Xue, Y.; Reif, B.; Skrynnikov, N. R. *J. Am. Chem. Soc.* **2008**, *130*, 16611). An equivalent assumption is made in the rDC-based studies, where interactions between protein and alignment media can potentially alter a protein's native dynamics (Louhivuori, M.; Otten, R.; Lindorff-Larsen, K.; Annila, A. *J. Am. Chem. Soc.* **2006**, *128*, 4371).
(18) Clore, G. M.; Driscoll, P. C.; Wingfield, P. T.; Gronenborn, A. M. *Biochemistry* **1990**, *29*, 7387.
(19) This statistics is slightly different from the one reported in ref 15 due to several corrected spectral assignments. The conclusions of the article remain unaffected.
(20) Chevelkov, V.; Fink, U.; Reif, B. *J. Biomol. NMR* **2009**, *45*, 197.
(21) Chevelkov, V.; Faelber, K.; Diehl, A.; Heinemann, U.; Oschkinat, H.; Reif, B. *J. Biomol. NMR* **2005**, *31*, 295.
(22) Brooks, B. R.; et al. *J. Comput. Chem.* **2009**, *30*, 1545.
(23) Xue, Y.; Pavlova, M. S.; Ryabov, Y. E.; Reif, B.; Skrynnikov, N. R. *J. Am. Chem. Soc.* **2007**, *129*, 6827.
(24) Brüschweiler, R.; Wright, P. E. *J. Am. Chem. Soc.* **1994**, *116*, 8426.
(25) Vega, M. C.; Martínez, J. C.; Serrano, L. *Protein Sci.* **2000**, *9*, 2322.
(26) Martinez, J. C.; Pisabarro, M. T.; Serrano, L. *Nat. Struct. Biol.* **1998**, *5*, 721.
(27) Krieger, F.; Fierz, B.; Bieri, O.; Drewello, M.; Kiefhaber, T. *J. Mol. Biol.* **2003**, *332*, 265.
(28) Ishima, R.; Freedberg, D. I.; Wang, Y. X.; Louis, J. M.; Torchia, D. A. *Structure* **1999**, *7*, 1047. Rozovsky, S.; McDermott, A. E. *J. Mol. Biol.* **2001**, *310*, 259.
(29) Mulder, F. A. A.; Mittermaier, A.; Hon, B.; Dahlquist, F. W.; Kay, L. E. *Nat. Struct. Biol.* **2001**, *8*, 932.
(30) Loria, J. P.; Rance, M.; Palmer, A. G. *J. Am. Chem. Soc.* **1999**, *121*, 2331. Eisenmesser, E. Z.; Millet, O.; Labeikovsky, W.; Korzhnev, D. M.; Wolf-Watz, M.; Bosco, D. A.; Skalicky, J. J.; Kay, L. E.; Kern, D. *Nature* **2005**, *438*, 117.
(31) Anfinsen, C. B. *Science* **1973**, *181*, 223.
(32) Davis, I. W.; Arendall, W. B.; Richardson, D. C.; Richardson, J. S. *Structure* **2006**, *14*, 265.

JA100645K

Supporting Information

Comparison of Solid-State Dipolar Couplings and Solution Relaxation Data Provides Insight into Protein Backbone Dynamics.

Veniamin Chevelkov,[†‡] Yi Xue,[‡] Rasmus Linser,[†] Nikolai R. Skrynnikov,[‡]*Bernd Reif[†]*

† *Forschunginstitut für Molekulare Pharmakologie (FMP), Robert-Rössle-Strasse 10, 13125 Berlin, Germany*

‡ *Department of Chemistry, Purdue University, 560 Oval Drive, W. Lafayette, Indiana 47907-2084*

nikolai@purdue.edu; reif@fmp-berlin.de

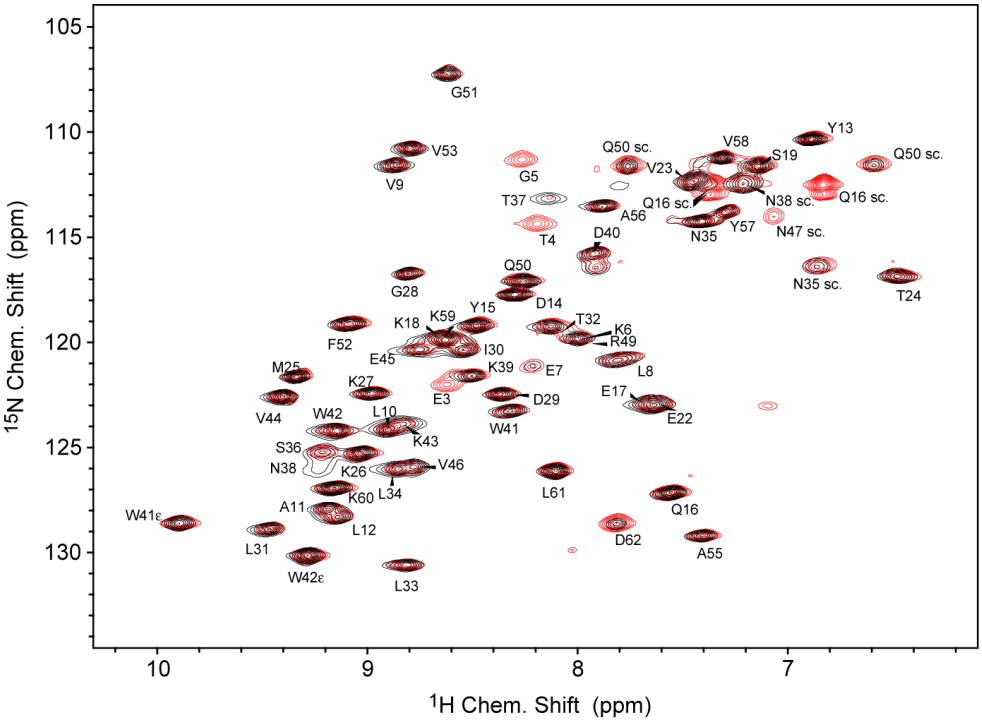

Figure S1. Two superimposed solid-state spectra of α-spectrin SH3 domain. Recorded by means of HSQC-style pulse sequences employing INEPT transfer elements (red contour lines) or, alternatively, CP transfer elements (black contour lines). Special effort has been made to acquire the data under identical conditions: $t_1^{max} = 93$ ms (400 increments, scalar coupling refocused using ^{1}H 180º composite pulse), $t_2^{max} = 80$ ms (WALTZ-16 ^{15}N decoupling, 2.5 kHz *rf* field strength), measurement time 2.5 h per spectrum. The spectra were recorded back-to-back using the protein sample with 25% content of back-exchanged protons, doped with 75 mM Cu-EDTA[1] at static magnetic field strength 600 MHz, MAS speed 24 kHz, temperature 22 ºC. Processing and plotting parameters for the two spectra are identical.

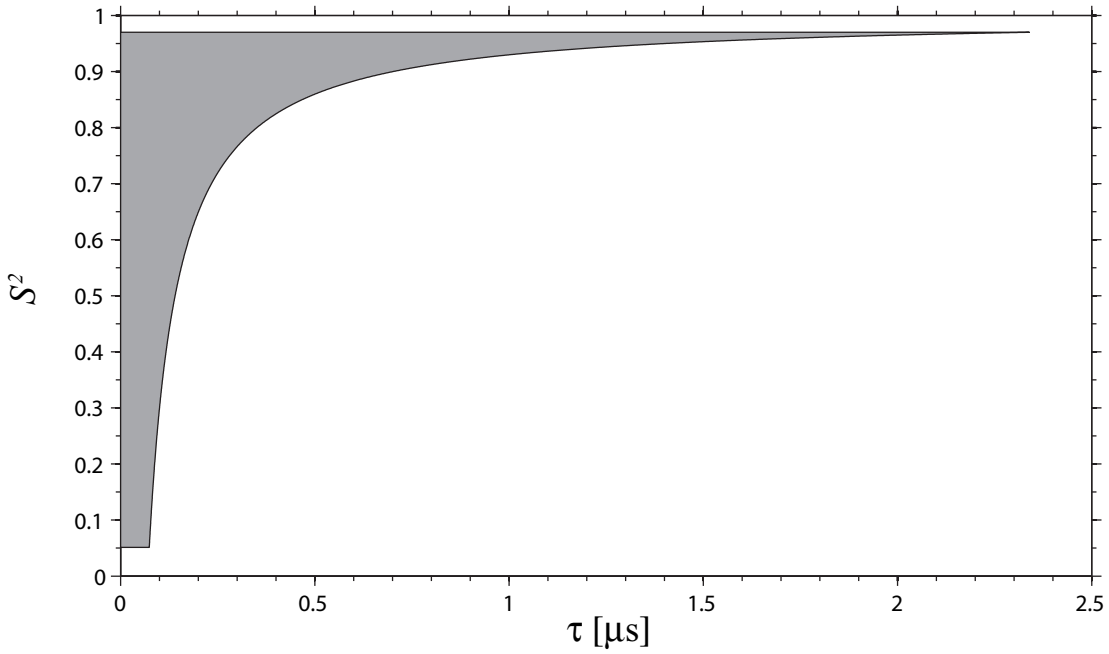

Figure S2. Range of dynamic parameters $\{S^2, \tau\}$ that can be probed by means of solid-state DC measurements (shaded area in the plot). The area is constrained by: (*i*) $S^2 = 0.97$ (at the current level of accuracy, higher S^2 values cannot be distinguished from 1.0), (*ii*) $S^2 = 0.05$ (lower S^2 values produce small DC constants that cannot be properly sampled using the current experimental scheme[2]), and (*iii*) the curve corresponding to $R_2 = 100$ s^{-1} (it is assumed that higher relaxation rates cause excessive line broadening). The above choice of boundaries is somewhat arbitrary and serves the purpose of illustration. In calculating R_2, we made use of the previous observations suggesting that Lipari-Szabo formalism is suitable for analysis of spin relaxation in solids:[3, 4]

$$R_2 = \frac{1}{20} c_{dip}^2 \{4J(0) + J(\omega_H - \omega_N) + 3J(\omega_N) + 3J(\omega_H) + 6J(\omega_H + \omega_N)\} + \frac{1}{20} c_{CSA}^2 \{4J(0) + 3J(\omega_N)\} \quad \text{(S1)}$$

where

$$J(\omega) = (1 - S^2)\frac{\tau}{1 + \omega^2 \tau^2}, \quad c_{dip} = -\frac{\mu_0}{4\pi}\frac{\gamma_H \gamma_N \hbar}{r_{NH}^3}, \quad \text{and} \quad c_{CSA} = \frac{2}{3}\gamma_N B_0 \Delta\sigma_N . \quad \text{(S2)}$$

The standard settings $r_{NH} = 1.02$ Å, $\Delta\sigma_N = -172$ ppm have been used in the computations, with static magnetic field strength $\gamma_H B_0 / 2\pi = 600$ MHz. The Redfield-theory expressions for spin relaxation are valid for the range of parameters covered, especially considering that only a fraction of the ^{1}H^N-^{15}N dipolar interaction is modulated by the internal protein motion. The time scale τ is sufficiently short so that the results do not need to be corrected for the effect of MAS.[5]

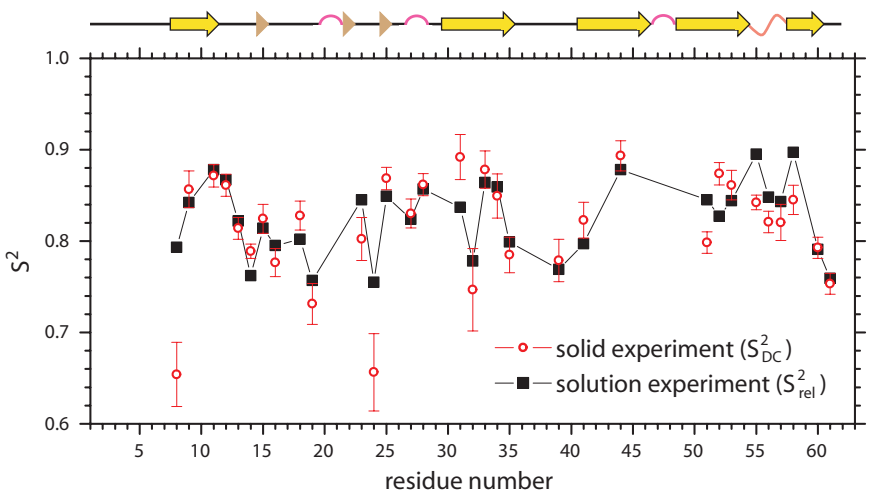

Figure S3. Experimentally determined order parameters in α-spectrin SH3. This plot is the equivalent of Fig.1 that additionally displays the estimated S^2_{DC} uncertainties. The error bars reflect the precision of the data, i.e. report on random errors; for discussion of small systematic errors see Chevelkov *et al.*[2] The secondary structure as determined by DSSP analysis[6] of 1U06 is: 8-11, 30-35, 41-46, 49-54 and 58-60 β-sheet, 55-57 3_{10}-helix, 20-21, 27-28, and 47-48 hydrogen-bonded turns, 15, 22, and 25 isolated β-bridges.

Residue number	S^2_{rel}	S^2_{DC}
2	(0.15)	-[a]
3	(0.19)	-[a]
4	(0.27)	-[a]
5	(0.27)	-[a]
6	(0.38)	-[a]
7	(0.62)	-[a]
8	0.79	0.65
9	0.84	0.86
10	0.87	-[b]
11	0.89	0.87
12	0.87	0.86
13	0.82	0.81
14	0.76	0.79
15	0.81	0.82
16	0.79	0.78
17	-[b]	-[b]
18	0.80	0.84
19	0.76	0.73
20	-[c]	-[c]
21	0.77	-[a]
22	0.87	-[b]
23	0.85	0.80
24	0.76	0.66
25	0.85	0.87
26	-[b]	0.84
27	0.82	0.83
28	0.86	0.86
29	0.89	0.87
30	-[b]	0.84
31	0.84	0.89
32	0.78	0.75

Residue number	S^2_{rel}	S^2_{DC}
33	0.86	0.88
34	0.86	0.85
35	0.80	0.78
36	0.82	-[a]
37	0.85	0.85
38	0.88	-[a]
39	0.77	0.79
40	0.81	0.84
41	0.80	0.82
42	0.82	0.86
43	0.83	-[b]
44	0.88	0.89
45	-[b]	0.84
46	-[b]	0.81
47	0.81	-[a]
48	-[a]	-[a]
49	-[b]	0.72
50	-[b]	0.71
51	0.85	0.80
52	0.83	0.87
53	0.84	0.86
54	-[c]	-[c]
55	0.90	0.84
56	0.85	0.82
57	0.84	0.82
58	0.90	0.84
59	-[b]	0.82
60	0.79	0.79
61	0.76	0.75
62	-[b]	0.35

Table S1. Experimentally measured relaxation-based and DC-based order parameters. The absent data are due to: (a) weak or missing peaks, (b) spectral overlaps, and (c) proline residues. The solution data from residues 2-7 have been analyzed using the extended, four-parameter version of Lipari-Szabo model.[7] All of these residues show substantial amount of motion on 1-2 ns time scale; reported in this table are the values of $S^2_{rel,f}S^2_{rel,s}$ (shown in brackets).

Order parameters and local dynamics.

1. *Isotropic local dynamics*

As a starting point in the discussion, let us assume that the local motion of an NH vector is characterized by a three-fold or higher symmetry. For instance, "diffusion in a cone" model that has axial symmetry (C_∞) fits this description.[8] It is straightforward to calculate the order parameters arising from this model. Considering relaxation experiments in solution, it is appropriate to use Eq. (1):

$$S^2 = (4\pi/5)\sum_{m=-2}^{2} < Y^*_{2m}(\theta,\varphi) >< Y_{2m}(\theta,\varphi) > \qquad \text{(S3)}$$

Here it is assumed that the tumbling of the molecule is isotropic, so that the directional angles of the NH vector (θ,φ) can be defined relative to an arbitrary molecular frame. Choosing a molecular frame such that its z axis lies along the axis of the cone, we obtain $< Y_{2m}(\theta,\varphi) >= 0$ for $m = \pm 1, \pm 2$. The order parameter is, therefore, reduced to $S^2 = (4\pi/5) < Y_{20}(\theta) >^2$. If local motion is much faster than the overall tumbling, then S^2 is equivalent to S^2_{rel} .

Considering dipolar coupling experiments in solids, it is convenient to start with the relevant Hamiltonian:

$$H_{dip} = c_{IS} 2 I_z S_z D^{L\leftarrow P}_{0,0}(0,\tilde{\theta},0) \qquad \text{(S4)}$$

where $c_{IS} = -(\mu_0/4\pi)\gamma_I\gamma_S\hbar/r^3_{IS}$, and $D^{L\leftarrow P}_{0,0}$ is the element of the second-rank Wigner matrix defined according to Haeberlen[9] that relates the principal axis frame P (z axis along the NH vector) to the laboratory frame L (z axis along the static magnetic field). To investigate the effect of the internal motion, H_{dip} needs to be rewritten as:

$$H_{dip} = c_{IS} 2 I_z S_z \sum_{p=-2}^{2} D_{p,0}^{L \leftarrow M}(0, \tilde{\tilde{\theta}}, 0) D_{0,p}^{M \leftarrow P}(\varphi, \theta, 0) \quad \text{(S5).}$$

Here we refer to the molecular frame M, which has its z axis along the axis of the cone. This frame is the same as used above in calculating S_{rel}^2, and the angles (θ, φ) have the same meaning. Assuming that the local motion is fast (in particular, faster than sample spinning in a MAS experiment), we can calculate the residual Hamiltonian that is partially averaged through the effect of the internal dynamics:

$$< H_{dip} >= c_{IS} 2 I_z S_z \sum_{p=-2}^{2} D_{p,0}^{L \leftarrow M}(0, \tilde{\tilde{\theta}}, 0) < D_{0,p}^{M \leftarrow P}(\varphi, \theta, 0) > \quad \text{(S6)}$$

As before, only the contribution with $p = 0$ survives, producing:

$$< H_{dip} >= c_{IS} 2 I_z S_z D_{0,0}^{L \leftarrow M}(0, \tilde{\tilde{\theta}}, 0) < D_{0,0}^{M \leftarrow P}(0, \theta, 0) > \quad \text{(S7)}$$

The above expression is equivalent to the original Hamiltonian Eq. (S4) aside from two aspects: (*i*) it implies that the NH vector is oriented along the axis of the cone of motion and (*ii*) it includes the factor $< D_{0,0}^{M \leftarrow P}(0, \theta, 0) >$ that effectively scales the interaction constant c_{IS}. This factor can be readily identified as DC order parameter and evaluated as follows: $S_{DC} =< D_{0,0}^{M \leftarrow P}(0, \theta, 0) >= (4\pi/5)^{1/2} < Y_{20}(\theta) >$. Thus, it becomes apparent that $S_{DC}^2 = S_{rel}^2$, consistent with the commonly made assumption.

Let us now consider the effect of internal dynamics on spin evolution under the conditions of CP recoupling in MAS experiment.[2] In principle, the existing results by Zilm and co-workers[10, 11] are applicable to this experiment if the constant c_{IS} is replaced with $c_{IS} S_{DC}$ (this follows from the fundamental similarity between Eq. (S4) and (S7)). Here we briefly illustrate the derivation of these results since it is relevant for the following discussion.

The Hamiltonian Eq. (S5) can be rewritten as:

$$H_{dip} = c_{IS} 2 I_z S_z \sum_{p,q=-2}^{2} D_{p,0}^{L \leftarrow R}(0, \beta_{MAS}, \omega_R t) D_{q,p}^{R \leftarrow M}(\alpha, \beta, \gamma) D_{0,q}^{M \leftarrow P}(\varphi, \theta, 0) \quad \text{(S8).}$$

Here R denotes the rotor frame, β_{MAS} is the magic angle, $\omega_R / 2\pi$ is the spinning speed, and (α, β, γ) define the transformation from the molecular frame to the rotor frame (in a polycrystalline sample, these angles are different for each individual crystallite). This result can be averaged with respect to the local motion (see above) and then rewritten using the explicit expressions for Wigner matrices:[9]

$$< H_{dip} >= c_{IS} 2 I_z S_z \sum_{p=-2}^{2} f_p \exp(ip\omega_R t) \quad \text{(S9).}$$

For the experiment with CP match at +1 (-1) spinning sideband,[2] the magnetization transfer is actuated by the coefficient f_1 (f_{-1}):[10]

$$| f_{\pm 1} |= \frac{\sqrt{2}}{4} S_{DC} | \sin 2\beta | \quad \text{(S10).}$$

Finally, the amplitude of the magnetization transfer associated with an individual crystallite is:[10]

$$S_x(t) \sim \sin^2\left(c_{IS} | f_{\pm 1} | \frac{t}{2} \right) \quad \text{(S11).}$$

In order to obtain the net signal, the result Eq. (S11) should be integrated over the surface of unit sphere (powder average). Note that the above treatment is rather basic. In particular, it neglects the effect of *rf* inhomogeneity and ^{15}N CSA interaction; it also makes no attempt to model the details of the actual pulse sequence.[2] Nevertheless, it is sufficient to form an idea about the role of local dynamics.

2. *Anisotropic local dynamics*

As an alternative scenario, let us now assume that the local motion lacks the C_n $(n \geq 3)$ symmetry. For example, let us examine a simple two-site jump model, where the NH vector hops between two (equally probable) orientations with the amplitude of the jump 2Φ. The relaxation order parameter for this model can be calculated in a straightforward fashion using Eq. (S3):[12]

$$S_{rel}^2 = 1 - (3/4) \sin^2 2\Phi \quad \text{(S12)}$$

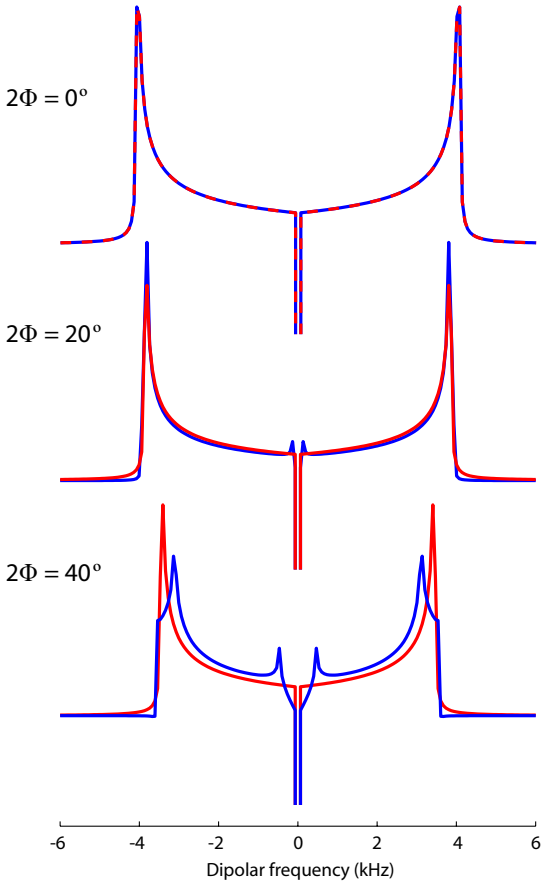

Figure S4. ^{15}N-^{1}H^{N} dipolar spectra simulated using the anisotropic model of local motion (Eqs. (S11) and (S14); blue traces) and the best fits of these simulated data using the isotropic model of local motion, (Eqs. (S11) and (S10); red traces). The fitting was performed by minimizing the *rms* deviation between the curves over the frequency interval from -6 to -0.5 kHz (0.5 to 6 kHz), which excludes the irrelevant spectral feature at zero frequency. The minimization was carried out using a grid search in a space of two parameters: S_{DC} and the overall signal amplitude.

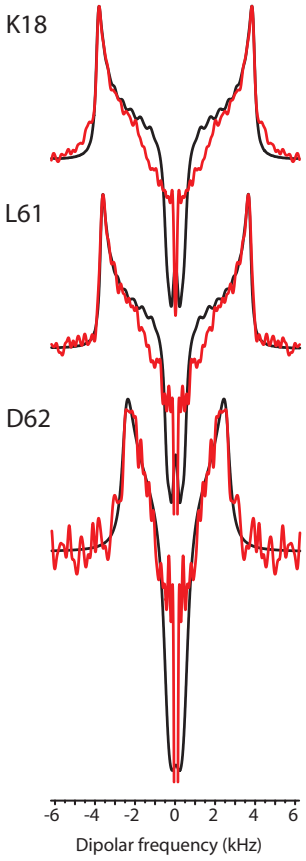

Figure S5. Experimental ^{15}N-^{1}H^{N} dipolar spectra of selected residues in α-spectrin SH3 domain (red traces) and best fits of these experimental data using the SIMPSON program[13] (black traces). Reproduced from Chevelkov *et al*.[2]

To analyze the solid-state experiment, it is convenient to cast the dipolar Hamiltonian in the following form:[3]

$$H_{dip}(\pm\Phi) = c_{IS}\, 2I_z S_z \sum_{p,q=-2}^{2} D_{p,0}^{L\leftarrow R}(0,\beta_{MAS},\omega_R t) D_{q,p}^{R\leftarrow M}(\alpha,\beta,\gamma) D_{0,q}^{M\leftarrow P}(\pm\Phi,\frac{\pi}{2},0) \qquad \text{(S13)}.$$

In this expression the molecular frame M is defined such that its z axis lies along the rotation axis of the two-site jump motion; the rotations by the amount $+\Phi$ and $-\Phi$ correspond to the two sampled NH orientations. The dynamic averaging, due to jumps between the two orientations, leads to $< H_{dip} >= (H_{dip}(\Phi) + H_{dip}(-\Phi))/2$. After some algebra, one obtains:

$$|f_{\pm 1}| = \frac{\sqrt{2}}{4} |\sin\beta| \sqrt{\cos^2\beta(1+\cos 2\gamma\cos 2\Phi)^2 + \sin^2 2\gamma\cos^2 2\Phi} \qquad \text{(S14)}$$

with Eq.(S11) describing the time evolution profile of an individual crystallite. To obtain the net signal, Eq. (S11) (complemented by Eq. (S14)) should be integrated over the surface of the unit sphere. The integration involves two angles, β and γ , instead of the single angle β in Eq. (S10). Indeed, there are two directional parameters in the present model: average orientation of the NH vector and the direction of the jump.

At this point we are prepared to investigate the potential impact of the motional anisotropy on the extracted values of S_{DC} . For this purpose, we simulated the DC time evolution profiles using Eq. (S14) and (S11) (the latter subject to powder averaging). The result was Fourier-transformed and the real part was retained, same as in our experimental procedure.[2] The resulting dipolar spectra are shown with blue lines in Fig. S4. The spectral pattern is obviously different from the generic shape (cf. top and bottom panels in Fig. S4). To understand why this is so, consider the NH vector that is oriented at a right angle to the rotor axis. If this vector jumps in the equatorial

plane then the effective dipolar coupling remains unchanged. Conversely, if the vector jumps in a meridional plane then the coupling is rescaled. This kind of behavior is responsible for the complex lineshapes observed in the simulations. The sensitivity of solid-state lineshapes to the details of local dynamics is a familiar phenomenon, especially well documented in the ^{2}H studies.[14]

The spectra simulated using the anisotropic model (two-site jumps) were subsequently fitted using the isotropic model (diffusion in a cone). The fits are represented by red traces in Fig. S4. As can be appreciated from the bottom panel in Fig. S4, the fitting criteria are open to discussion. In our simulations, we sought to minimize the *rms* deviation between the two spectral traces. Alternatively, one may seek to reproduce the distinctive spectral features, such as position of the 'horns'. With our fitting routine we were able to recover the S^2 values quite well. For example, for the jump amplitude $2\Phi = 20°$ the target order parameter is $S^2_{rel} = 0.91$ (see Eq. (S12)). At the same time, when the isotropic model is used to fit the simulated dipolar spectrum, the extracted order parameter is $S^2_{DC} = 0.90$. For the jump amplitude $2\Phi = 40°$ the corresponding numbers are 0.69 and 0.72.

In assessing the results in Fig. S4 one should keep in mind several considerations. First, the model where NH vector jumps by 40° almost certainly exaggerates the anisotropic character of motion. In reality, the motion of the NH vectors is usually fairly close to isotropic.[15] Second, as already mentioned, the simulations in Fig. S4 are simplistic in that they do not take into account ^{15}N CSA, *rf* inhomogeneity, proton relaxation, details of the actual pulse sequence, etc. When all these additional variables are included, the detection of motional anisotropy will likely become more difficult. Third, the experimental spectra have limited signal-to-noise ratio and resolution (illustrated in Fig. S5). This makes the detection of motional anisotropy even more problematic. Based on all these observations, we conclude that there is no support for use of the anisotropic model in the present study.

MD simulation protocol

The starting coordinates for the solid-state MD trajectory were obtained from the high-resolution crystallographic structure 1U06.[16] This structure misses six N-terminal residues and one C-terminal residue. As discussed in the text, the N-terminal region is significantly disordered in the crystalline state and undergoes a nanosecond time scale conformational exchange. Given that the terminal residues are absent from the crystallographic structures (as well as solid-state NMR structure[17]), it is necessary to model these residues while taking into consideration the effects of crystal packing.

Toward this goal, we produced 150 structural models based on 1U06 geometry, where the terminal segments were initially generated in a form of random coil[18] and appended to the body of the protein. The resulting constructs were packed into a unit cell (space group $P2_12_12_1$, four protein molecules per cell). The dimension of the unit cell, $34.47 \times 42.48 \times 50.80$ Å , were taken from a room-temperature crystallographic structure 2NUZ. The cells were subsequently hydrated using the standard facilities of the CHARMM program.[19]

As a next step, the coordinates of the terminal residues were optimized for each model using the protocol adapted from Sali et al.[20] To emulate crystal lattice environment, periodic boundary conditions have been applied at the faces of the unit cell. All heavy atoms in protein molecules, except those in six N-terminal residues and one C-terminal residue, have been fixed. The optimization procedure, implemented in CHARMM (version 32b2, CHARMM22 force field), begins with 500 steps of steepest descent minimization, followed by 500 steps of adopted basis Newton-Raphson minimization. The system is then heated from 100 to 1000 K with a step of 225 K and subsequently cooled back to 100 K (integration time step 1 fs, other parameters as described by Xue et al.[21]; total duration of the heating and cooling stages is 4 and 12 ps, respectively). Finally, the model is subjected to 200 rounds of Powell minimization.

The 150 optimized models were ranked according to energy and the lowest-energy model was chosen as a starting point for the MD production run.* The described MD setup rigorously accounts for all crystal contacts formed by α-spectrin SH3 in the orthorhombic cell. In the selected lowest-energy model, each protein molecule makes contacts with 6 neighboring molecules and 35% of the solvent accessible surface area is occupied by crystal contacts.

The MD simulation protocol was the same as used previously to generate the 30-ns trajectory of α-spectrin SH3 in solution.[7, 21] The only difference concerns the definition of the water box and the associated periodic boundary conditions (PBCs). In the case of the solid-state simulation, the PBCs are intended to recreate the crystal lattice environment, including multiple crystal contacts. In solution, on the other hand, the water box is constructed to ensure that the protein is surrounded by a sufficiently thick water shell which prevents direct contacts between the protein and its PBC image.

The 50-ns solid-state MD trajectory was recorded in ca. 2 months using one GNU/Linux workstations equipped with a pair of 3-GHz dual-core Xeon processors. Given that the simulation involves 4 protein molecules contained in the crystal unit cell, the actual statistics is better than suggested by the nominal length of the trajectory. The convergence can be judged from the spread in the simulated S^2_{DC} values (pink shaded area in Fig. 2 of the text). The trajectories were processed as described previously.[21] An attempt to eliminate small-amplitude reorientational motions (i.e. 'rocking' of protein molecules in the crystal lattice) had virtually no impact on the extracted order parameters. In the final protocol the simulated solid-state data were treated as is, with no attempt to eliminate any motional modes.

The previously described solution trajectory[7, 21] has been extended to the total length of 50 ns in order to match the length of the solid-state trajectory.

* As a control, we have chosen another low-energy model, showing a different conformation of the N-terminus, and recorded a 30-ns trajectory starting with this alternative model. The results proved to be similar and are not reported in this paper.

References

(1) Linser, R.; Chevelkov, V.; Diehl, A.; Reif, B. J. Magn. Reson. 2007, 189, 209.
(2) Chevelkov, V.; Fink, U.; Reif, B. J. Am. Chem. Soc. 2009, 131, 14018.
(3) Skrynnikov, N. R. Magn. Reson. Chem. 2007, 45, S161.
(4) Agarwal, V.; Xue, Y.; Reif, B.; Skrynnikov, N. R. J. Am. Chem. Soc. 2008, 130, 16611.
(5) Farès, C.; Qian, J.; Davis, J. H. J. Chem. Phys. 2005, 122.
(6) Kabsch, W.; Sander, C. Biopolymers 1983, 22, 2577.
(7) Chevelkov, V.; Zhuravleva, A. V.; Xue, Y.; Reif, B.; Skrynnikov, N. R. J. Am. Chem. Soc. 2007, 129, 12594.
(8) Richarz, R.; Nagayama, K.; Wuthrich, K. Biochemistry 1980, 19, 5189.
(9) Haeberlen, U., High resolution NMR in solids. Selective Averaging. In Advances in Magnetic Resonance, Suppl. 1, Waugh, J. S., Ed., Academic Press: New York, 1976.
(10) Wu, X. L.; Zilm, K. W. J. Magn. Reson. Ser. A 1993, 104, 154.
(11) Paulson, E. K.; Martin, R. W.; Zilm, K. W. J. Magn. Reson. 2004, 171, 314.
(12) Daragan, V. A.; Mayo, K. H. J. Magn. Reson. Ser. B 1995, 107, 274.
(13) Bak, M.; Rasmussen, J. T.; Nielsen, N. C. J. Magn. Reson. 2000, 147, 296.
(14) Spiess, H. W. Adv Polym Sci 1985, 66, 23; Hoatson, G. L.; Vold, R. L., 2H NMR spectroscopy of solids and liquid crystals. In NMR Basic Principles and Progress, Diehl, P.; Fluck, E.; Gunther, H.; Kosfield, R.; Seelig, J., Ed., Springer-Verlag: Berlin, 1994; 32, 1; Hologne, M.; Faelber, K.; Diehl, A.; Reif, B. J. Am. Chem. Soc. 2005, 127, 11208.
(15) Lienin, S. F.; Bremi, T.; Brutscher, B.; Bruschweiler, R.; Ernst, R. R. J. Am. Chem. Soc. 1998, 120, 9870; Yao, L.; Vögeli, B.; Torchia, D. A.; Bax, A. J. Phys. Chem. B 2008, 112, 6045.
(16) Chevelkov, V.; Faelber, K.; Diehl, A.; Heinemann, U.; Oschkinat, H.; Reif, B. J. Biomol. NMR 2005, 31, 295.
(17) Castellani, F.; van Rossum, B.; Diehl, A.; Schubert, M.; Rehbein, K.; Oschkinat, H. Nature 2002, 420, 98.
(18) Feldman, H. J.; Hogue, C. W. V. Proteins: Struct. Funct. Genet. 2000, 39, 112.
(19) Brooks, B. R.; Brooks, C. L.; Mackerell, A. D.; Nilsson, L.; Petrella, R. J.; Roux, B.; Won, Y.; Archontis, G.; Bartels, C.; Boresch, S.; Caflisch, A.; Caves, L.; Cui, Q.; Dinner, A. R.; Feig, M.; Fischer, S.; Gao, J.; Hodoscek, M.; Im, W.; Kuczera, K.; Lazaridis, T.; Ma, J.; Ovchinnikov, V.; Paci, E.; Pastor, R. W.; Post, C. B.; Pu, J. Z.; Schaefer, M.; Tidor, B.; Venable, R. M.; Woodcock, H. L.; Wu, X.; Yang, W.; York, D. M.; Karplus, M. J. Comput. Chem. 2009, 30, 1545.
(20) Fiser, A.; Do, R. K. G.; Sali, A. Protein Sci 2000, 9, 1753.
(21) Xue, Y.; Pavlova, M. S.; Ryabov, Y. E.; Reif, B.; Skrynnikov, N. R. J. Am. Chem. Soc. 2007, 129, 6827.